JCI insight

Adipsin and Adipocyte-derived C3aR1 Regulate Thermogenic Fat in a Sex-dependent Fashion

Lunkun Ma, … , Liling Tang, James C. Lo

JCI Insight. 2024. https://doi.org/10.1172/jci.insight.178925.

Research In-Press Preview Inflammation Metabolism

Graphical abstract

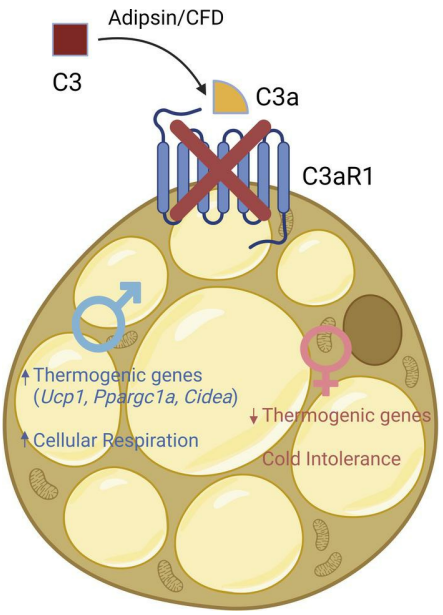

Adipsin and Adipocyte-derived C3aR1 Regulate Thermogenic Fat in a Sex-dependent Fashion

Lunkun Ma[1,2,3,4], Ankit Gilani[1,2,3], Alfonso Rubio-Navarro[1,2,3], Eric Cortada[1,2,3], Ang Li[1,2,3], Shannon M. Reilly[1,2], Liling Tang[4]*, James C. Lo[1,2,3]*.

1. Division of Cardiology, Department of Medicine, Weill Cornell Medicine, New York, NY, USA.
2. Weill Center for Metabolic Health, Weill Cornell Medicine, New York, NY, USA.
3. Cardiovascular Research Institute, Weill Cornell Medicine, New York, NY, USA.
4. Key Laboratory of Biorheological Science and Technology, Ministry of Education, College of Bioengineering, Chongqing University, Chongqing, China.

∗Correspondence: J.C.L.- 413 East 69th St, New York, NY 10021, 646-962-2038, jlo@med.cornell.edu; tangliling@cqu.edu.cn

Conflict of interest

The authors have declared that no conflict of interest exists.

Abstract

Thermogenesis in beige/brown adipose tissues can be leveraged to combat metabolic disorders such as type 2 diabetes and obesity. The complement system plays pleiotropic roles in metabolic homeostasis and organismal energy balance with canonical effects on immune cells and non-canonical effects on non-immune cells. The adipsin/C3a/C3aR1 pathway stimulates insulin secretion and sustains pancreatic beta cell mass. However, its role in adipose thermogenesis has not been defined. Here, we show that male *Adipsin/Cfd* knockout mice exhibit increased energy expenditure and white adipose tissue (WAT) browning. In addition, male adipocyte-specific *C3aR1* knockout mice exhibit enhanced WAT thermogenesis and increased respiration. In stark contrast, female adipocyte-specific *C3aR1* knockout mice display decreased brown fat thermogenesis and are cold intolerant. Female mice express lower levels of *Adipsin* in thermogenic adipocytes and adipose tissues than males. *C3aR1* is also lower in female subcutaneous adipose tissue than males. Collectively, these results reveal sexual dimorphism in the adipsin/C3a/C3aR1 axis in regulating adipose thermogenesis and defense against cold stress. Our findings establish a newly discovered role of the alternative complement pathway in adaptive thermogenesis and highlight sex-specific considerations in potential therapeutic targets for metabolic diseases.

Key Words: Thermogenesis; Complement, Adipsin; C3aR1; Adipocyte

Introduction

Obesity remains a serious global public health problem that greatly increases the risk of type 2 diabetes (T2D) and other associated diseases, including cardiovascular disease and many types of cancer (1, 2). Bariatric surgery, currently the most effective durable option for treating severe obesity carries risk of surgical complications, death, and reoperation (3). Glucagon-like peptide 1 receptor (GLP-1R) and gastric inhibitory polypeptide 1 receptor (GIP-R) dual agonists are the most promising medical treatments for obesity to date, largely dependent on suppressing food intake (4, 5). Adaptive thermogenesis, the production of heat by the body in response to stimuli such as cold, is considered a promising therapeutic approach to counteract obesity (6). Thermogenic adipocytes in the brown and white adipose tissue depots are specialized cells that are responsible for adaptive thermogenesis through uncoupling protein 1 (UCP1) enhancing the leakage of protons across the mitochondrial membrane and other futile cycling pathways (7-9). Beige adipocytes embedded in white adipose tissues have multilocular lipid droplets and can promote thermogenesis like brown adipocytes (9, 10). Beige adipocytes can arise from both preadipocyte progenitors and pre-existing mature unilocular white adipocytes (9, 11-15). The formation of beige adipocytes is activated by cold exposure, β-adrenergic stimulation, and other stimuli (9). The detection of brown adipose tissue (BAT) in human adults has further piqued interest in enhancing energy expenditure by increasing the thermogenic activity of brown and beige adipocytes (16-18). However, therapies to stimulate the thermogenic capacity of adipose tissues based on cold exposure or β-adrenergic agonists remain clinically challenging. Therefore, there

is considerable interest in finding new mechanisms that promote browning and enhance thermogenesis in adipose.

The complement system consists of many distinct complement components that interact with one another. As an important part of the innate immune system, complement plays a key role in the defense against common pathogens (19). A growing body of research suggests that certain components of the complement system also play an important role in the regulation of metabolic disorders such as diabetes and insulin resistance (20-22). A critical complement component, complement factor D, also known as adipsin, is mainly secreted by adipocytes. Adipocytes synthesize the major components of the alternative complement pathway, but the role complement plays in adipose tissue homeostasis is unknown. Adipsin controls the alternative complement pathway by catalyzing the production of the C3 convertase, which then cleaves C3 to generate C3a and C3b (23). We previously showed that C3a acts to increase beta cell insulin secretion, an effect that is dependent on C3a receptor 1(C3aR1) (21, 24). Several studies show marked though opposing roles of adipsin and C3aR1 on systemic glucose homeostasis in diet-induced obesity (20, 21, 25). These results suggest that there may be different cell-specific effects of adipsin/C3aR1 on obesity and diabetes. C3aR1 is predominantly expressed on immune cells and was not previously known to be expressed by adipocytes. Furthermore, it is unknown whether the adipsin/C3a/C3aR1 axis is involved in the regulation of systemic energy homeostasis and adipose thermogenesis.

In the present study, we show that *Adipsin/Cfd* deficiency increased the thermogenic program in white adipose tissue (WAT) under ambient conditions and with cold exposure. We find that adipocytes express the anaphylatoxin receptor C3aR1. We generated

adipocyte-specific *C3aR1* knockout (Ad-*C3aR1*$^{-/-}$) mice to elucidate the physiological roles of C3aR1 in adipocytes. Our study demonstrated that Ad-*C3aR1*$^{-/-}$ male mice exhibited enhanced thermogenic gene expression in subcutaneous adipose tissue. Male Ad-*C3aR1*$^{-/-}$ mice also showed increased heat production in thermogenic adipose tissue. Further in vitro studies showed that deletion of *C3aR1* in primary subcutaneous adipocytes from male mice enhanced thermogenic gene expression and mitochondrial respiration. Notably, we found sexual dimorphism in *Adipsin* and *C3aR1* gene expression. *Adipsin* was lower in both adipose tissue and thermogenic adipocytes of female mice compared to males. Subcutaneous adipose tissue *C3aR1* gene expression was also diminished in female mice compared to males. Furthermore, adipocyte-specific *C3aR1* knockout female mice produce less heat in their brown adipose tissues (BAT) and are cold intolerant compared to controls. Our results reveal the function of the adipsin/C3a/C3aR1 axis as a regulator of adipose thermogenesis and energy metabolism in a sex-dependent manner.

Results

Loss of Adipsin Leads to Increased Energy Expenditure and Protection from Diet-induced Obesity

We previously found that adipsin positively regulates adipose tissue inflammation in mice fed a high fat diet (HFD) (21). However, adipsin-deficient mice were mildly resistant to diet-induced obesity. To explore the potential role of adipsin in regulating whole-body energy homeostasis with metabolic stress, we compared the body weights of male wild type (WT) and *Adipsin*$^{-/-}$ mice fed a regular diet (RD) or HFD. As expected, *Adipsin* mRNA levels were noticeably absent in all the fat tissues of the knockout (KO) mice (Supplemental Figure 1A). While no change was seen in body weights between male WT and *Adipsin*$^{-/-}$ mice (Supplemental Figure 1B) on a regular diet, *Adipsin*$^{-/-}$ mice displayed a mild-moderate but significant reduction in body weight starting two months after HFD compared to both WT and *Adipsin*$^{+/-}$ mice (Figure 1A). Body composition analysis showed that the reduced weight gain of *Adipsin*$^{-/-}$ mice was mainly due to decreased fat mass without significant differences between WT and *Adipsin*$^{+/-}$ mice (Figure 1B). As body weight is determined by a balance between energy expenditure and energy intake, we assessed food intake and energy expenditure in *Adipsin*$^{-/-}$ and control mice at 4 weeks of HFD, before changes in body weight. Our results indicate that food intake was comparable between male WT and *Adipsin*$^{-/-}$ mice (Figure 1C), suggesting that the reduced body weight gain in *Adipsin*$^{-/-}$ mice was caused by increased energy expenditure. Indeed, *Adipsin*$^{-/-}$ mice exhibited an increase in O_2 consumption and CO_2 production compared to WT mice without significant differences in activity (Figure 1, D and E and Supplemental Figure 1, C-E).

Adipsin Deficiency Results in Enhanced Thermogenesis in White Fat

Since brown/beige adipocyte thermogenesis plays a key role in driving energy expenditure and adipsin is produced by adipocytes, we next examined whether there was enhanced adipose thermogenesis in *Adipsin*$^{-/-}$ mice. Ablation of adipsin resulted in increased expression of key thermogenic genes *Ucp1*, *Ppargc1a*, *Ppargc1b,* and *Prdm16* at room temperature in visceral (VISC) white adipose tissue (WAT) (Figure 2A) along with elevated *Ucp1* in subcutaneous (SubQ) WAT (Figure 2B). There was not a significant difference in thermogenic gene expression in the BAT between WT and *Adipsin*$^{-/-}$ mice (Supplemental Figure 2A).

SubQ WAT is prone to browning upon cold stimulation or β-adrenergic agonists (26). To further study the role of adipsin in regulation of white fat browning, we examined the effects of cold exposure on *Adipsin*$^{-/-}$ and WT mice. *Adipsin*$^{-/-}$ mice were similarly cold tolerant as controls (Supplemental Figure 2B). *Ucp1* was induced by 3-fold in the SubQ and VISC WAT of *Adipsin*$^{-/-}$ compared to WT mice following acute cold exposure (Figure 2C and Supplemental Figure 2C). However, the expression of thermogenic genes was not altered in the BAT of acute cold-exposed *Adipsin*$^{-/-}$ mice (Supplemental Figure 2D). Because of growing evidence that beige fat also uses alternative thermogenic pathways to dissipate energy in the form of heat(9), we next examined changes in *Ucp1*-independent thermogenic genes upon cold stimulation of SubQ fat. The *Adipsin*$^{-/-}$ group showed mild-moderately elevated expression of *Ldhb* and *Pkm* compared to controls (Supplemental Figure 2E). Consistent with the gene expression data, SubQ WAT from *Adipsin*$^{-/-}$ compared to that from WT mice showed more UCP1+ cells and reduced lipid

stores (Figure 2D). After 1 week of chronic cold exposure, we did not detect differences in thermogenic gene expression between WT and *Adipsin*$^{-/-}$ mice (Supplemental Figure 2, F-H).

Since adipsin and its products can potentially act on many different cell types, we next examined whether the increased numbers of thermogenic adipocytes in SubQ adipose tissue of *Adipsin*$^{-/-}$ mice was cell autonomous. Adipocytes differentiated in vitro from the SubQ adipose depot from *Adipsin*$^{-/-}$ mice also displayed a 4-5 fold increase in the expression of *Ucp1* and cell death inducing DFFA like effector A (*Cidea*) compared to controls (Figure 2E), suggesting an adipocyte cell-autonomous role for adipsin in thermogenesis. Furthermore, this increased expression of thermogenic genes in *Adipsin*$^{-/-}$ cells was also enhanced by the β-agonist isoproterenol (Figure 2E).

Adipsin catalyzes the formation of the C3 convertase, which can then result in the cleavage of C3 into C3a and C3b (21, 23). C3a acts on cells through its G-protein coupled receptor (GPCR) C3aR1 whereas C3b activates the C5 convertase that can result in formation of the C5b-C9 membrane attack complex (21, 27-29). To determine whether adipsin regulates subcutaneous adipocyte browning acutely through its downstream C3a/C3aR1 signaling pathway, we next assessed primary subcutaneous adipocytes from WT and *C3aR1* whole-body KO mice. We found that subcutaneous adipocytes from *C3aR1* KO mice differentiated in vitro showed a robust increase in the expression of thermogenic genes compared to WT controls (Figure 2F). Stimulating these cells with isoproterenol further augmented thermogenic gene expression in both groups with *C3aR1* KO adipocytes remaining 3-5 fold higher than controls (Figure 2F). These data suggest that adipsin through C3a/C3aR1 signaling regulates a browning phenotype in

subcutaneous adipocytes. However, we did not observe baseline differences in O_2 consumption and CO_2 production in *C3aR1*$^{-/-}$ compared to WT mice (Supplemental Figure 2, I and J).

Adipocyte C3aR1 Regulates Subcutaneous Adipocyte Thermogenic Gene Expression and Mitochondrial Respiration

To directly interrogate the role of C3aR1 on adipocytes in adaptive thermogenesis, we generated adipocyte specific C3aR1 KO mice by crossing *C3ar1* floxed mice with Adiponectin-Cre transgenic mice (Ad-*C3aR1*$^{-/-}$). Because of the cellular heterogeneity in adipose tissues with macrophages and immune cells expressing high levels of C3aR1, we analyzed *C3ar1* gene expression in the adipocyte fraction to confirm the adipocyte specific knockout in this system. Our results showed 50-65% knockdown of *C3ar1* in adipocytes in Ad-*C3aR1*$^{-/-}$ compared to controls (Figure 3A). Subcutaneous adipocytes from male Ad-*C3aR1*$^{-/-}$ mice showed a robust 4-fold increase in *Ucp1* and 2-fold increase in *Cidea* compared to controls (Figure 3B). Stimulation of these cells with isoproterenol further augmented thermogenic gene expression, especially in adipocytes lacking C3aR1 (Figure 3B). The increased expression of thermogenic genes in *C3aR1* knockout SubQ adipocytes prompted us to investigate the respiratory activity of isolated adipocytes from control and adipocyte specific *C3aR1* KO mice. Subcutaneous adipocytes from Ad-*C3aR1*$^{-/-}$ mice displayed double the maximal respiratory capacity and 50% more isoproterenol-stimulated respiration that was mostly due to uncoupled respiration but also with elevated Adenosine triphosphate (ATP)-coupled respiration (that sensitive to oligomycin) compared to controls (Figure 3, C-G). In the subcutaneous adipose tissue,

Ppargc1a was increased with similar trends in *Ucp1* and *Cidea* in male Ad-*C3aR1*$^{-/-}$ mice (Figure 3H). In contrast, brown adipocytes from control and Ad-*C3aR1*$^{-/-}$ did not show any significant differences in thermogenic gene expression nor mitochondrial respiration in response to isoproterenol (Supplemental Figure 3, A-F). There were also no differences in thermogenic gene expression between control and Ad-*C3aR1*$^{-/-}$ brown and visceral adipose tissues in the male mice (Supplemental Figure 3, G and H). UCP1 protein levels were also not affected in male Ad-*C3aR1*$^{-/-}$ brown and subcutaneous fat compared to controls (Supplemental Figure 3, I and J). These results suggest that C3aR1 on adipocytes regulates thermogenic gene expression and mitochondrial respiration mostly in subcutaneous but not brown adipocytes.

Given our findings of enhanced thermogenesis in subcutaneous but not brown adipocytes in the Ad-*C3aR1*$^{-/-}$ mice, we challenged male mice to cold and observed a modest improvement in cold tolerance in the KO mice (Figure 3I). There was no difference in body weight between the two groups before and after the cold challenge (Supplemental Figure 3K). We further measured heat production directly from the subcutaneous and brown fat ex vivo using CalScreener. We found a mild trend towards increased heat production in the brown but not subcutaneous fat of male Ad-*C3aR1*$^{-/-}$ mice compared to controls (Supplemental Figure 3, L and M). Together these results suggest a mild effect of improved adipose thermogenesis and cold tolerance with *C3ar1* ablation in adipocytes.

Sex-associated Differences in the Alternative Complement Pathway

Clinical studies have illuminated sex differences in alternative complement pathway activity but not in the classical and lectin pathways (30). The circulating levels of two important alternative complement components, C3 and adipsin, show sex-dependent differences (30, 31). These sex differences in humans prompted us to investigate if there is a similar sexual dimorphism in mice. We found no difference in circulating adipsin levels between male and female mice (Figure 4A). Since adipsin is predominantly secreted by adipose tissues, we assayed *Adipsin* and *C3aR1* levels in adipose tissues of male and female mice. We found that *Adipsin* mRNA level is lower in the thermogenic adipose tissue of female mice, especially in SubQ adipose tissue (Figure 4, B-D). However, *C3aR1* was only decreased in the SubQ adipose tissue of female mice compared with males (Figure 4B). *C3aR1* gene expression was not different between female and male mice in the visceral adipose tissue and BAT (Figure 4, C and D). Next, we assessed *Adipsin* mRNA levels in the adipocyte fractions from the different major fat depots. Our results show that *Adipsin* was significantly lower in subcutaneous and brown adipocytes of female mice compared with males (Figure 4E). These results reveal that there is sexual dimorphism in *Adipsin* expression in SubQ and brown but not visceral adipocytes in mice.

Ad-*C3aR1*$^{-/-}$ Female Mice Display Decreased Thermogenic Gene Expression and Cold Intolerance

Since we observed differences in expression of alternative pathway components between male and female mice, we tested if adipocyte C3aR1 expression may have different effects in female mice. In stark contrast to male mice, Ad-*C3aR1*$^{-/-}$ female mice exhibited substantial impairments at defending their core body temperature during acute

cold stress compared to controls without any changes in body weights (Figure 5A and Supplemental Figure 4A). We found that *Ppargc1b* and *Ckb* were mildly decreased with similar trends for *Prdm16* and *Ucp1* in the BAT of Ad-*C3aR1*$^{-/-}$ female mice compared to the control group during acute cold stress (Figure 5B). At room temperature, there was a similar trend of lower *Ucp1* in the BAT of Ad-*C3aR1*$^{-/-}$ female mice compared to controls (Supplemental Figure 4B). Thermogenic gene expression was not lower with *Serca2b* and *Ryr2* being elevated in the SubQ fat of Ad-*C3aR1*$^{-/-}$ compared to controls during acute cold exposure (Supplemental Figure 4C). Brown and subcutaneous fat UCP1 protein was also ~30% lower in Ad-*C3aR1*$^{-/-}$ female knockout mice compared to controls (Figure 5, C and D). Importantly, we observed 30% less heat production in the BAT without changes in SubQ fat of Ad-*C3aR1*$^{-/-}$ female mice compared to controls (Figure 5E and Supplemental Figure 4D). These results suggest that impaired BAT thermogenesis in Ad-*C3aR1*$^{-/-}$ female mice substantially compromised their endothermic response to acute cold exposure. We did not detect any gross differences in brown adipocyte morphology and lipid stores in the BAT between the two groups (Supplemental Figure 4E). Consistent with the changes in thermogenic gene expression, UCP1 staining was also fainter in the BAT of female Ad-*C3aR1*$^{-/-}$ mice compared to controls (Supplemental Figure 4F). Differentiated subcutaneous adipocytes from female Ad-*C3aR1*$^{-/-}$ mice did not show the same gene expression phenotype (Supplemental Figure 4G) in vitro as male Ad-*C3aR1*$^{-/-}$ adipocytes (Figure 3B), suggesting cell-intrinsic differences between sexes. While in vitro differentiated brown adipocytes from female Ad-*C3aR1*$^{-/-}$ mice did not exhibit the enhanced thermogenic gene expression seen in vivo with the BAT in female Ad-*C3aR1*$^{-/-}$ mice, suggesting critical in vivo inputs (Supplemental Figure 4H). Collectively, these

results indicate that adipocyte C3aR1 in female mice is critical for adaptive thermogenesis in the classical brown fat and defense against cold.

Discussion

Adipose tissues can synthesize the major components of the alternative complement pathway and are also one of the targets of complement activation in an autocrine or paracrine fashion (23). Although alternative complement activation is thought to promote the pathological progression of obesity-related metabolic diseases, the precise physiological mechanisms linking alternative complement pathways to metabolic dysfunction are not well defined. Here, we provide an essential role of the alternative complement adipsin/C3a/C3aR1 signaling axis in the cold-induced browning of white adipocytes. Deletion of *Adipsin* or *C3ar1* increases subcutaneous adipocyte thermogenic gene expression, resulting in adipocyte browning in cold-exposed male mice. Subcutaneous adipocytes lacking C3aR1 also demonstrate higher respiration rates though it remains to be determined which thermogenic pathway(s) or a combination thereof are responsible for the phenotype, including Serca2b/Ryr2 and glycolytic pathways that were mildly changed in some of our studies (32, 33). With UCP1 deficiency, UCP1-independent pathways can compensate (34, 35). It is also important to note that our studies tested C3aR1 KO but not in combination with UCP1, Creatine Kinase B (CKB) or tissue non-specific alkaline phosphatase (TNAP) KO (36, 37).

We demonstrate sexual dimorphism in the expression of *Adipsin* and *C3ar1*, key alternative complement components in adipose tissues. When and how the sex differences in gene expression manifest are an important questions worthy of future research. It is unknown if the sex-biased gene expression arise early during development, is dependent on sex hormones, or may be cell-type or organ specific. Critically, the effect of adipocyte specific C3aR1 deficiency on adipocyte browning are diametrically opposite

between male and female mice. Here we provide a rare molecular example of a non-sex hormone that regulates thermogenic adipose function in a sex-dependent fashion. Although it is unclear how much sex differences have been ignored in the past, our study highlights the importance of assessing for potential sexual dimorphism in adipose biology. C3a/C3aR1 seems to inhibit browning in males while stimulating adipocyte thermogenesis in female mice. This could be due to different tonicity of C3aR1 signaling between sexes, other external inputs, and/or the intrinsic differences in the C3aR1 signaling pathway between male and female beige adipocytes. Notably, we observe differences between *Adipsin*$^{-/-}$ and Ad-*C3ar1*$^{-/-}$ female mice with only the latter showing cold intolerance. A likely explanation for the discrepancy is that *Adipsin*$^{-/-}$ mice still express C3aR1 and there are other ligands for C3aR1 (e.g., TLQP-21) and other means of generating C3a such as with C3 tickover. The functional contributions of each of the thermogenic pathways whether UCP1-dependent or UCP1-independent in beige or brown adipocytes are outstanding questions for the field. How the downstream C3aR1 signaling pathway in adipocytes may differ between male and female mice will be of great future interest. It is noteworthy that autoimmune complement diseases in humans also display sexual dimorphism (31).

External stimuli can be leveraged to offset metabolic diseases by activating thermogenesis in brown and beige adipose tissues (38). Adipsin is the rate-limiting enzyme in the alternative pathway and controls downstream products such as C3a, C3b, and C5a (39). Our data suggest that the SubQ beige and brown adipocytes are a major target of adipsin/C3a through C3aR1. During complement activation, adipsin catalyzes the formation of the C3 convertase. C3 is highly abundant, but C3a is quickly converted

by carboxypeptidase B or N into the inactive C3a-desArg45 that does not signal through C3aR1 (20, 40). Indeed, the data here suggest that *C3aR1* deficiency significantly upregulated thermogenesis and mitochondrial respiration in male subcutaneous adipocytes. On the other hand, C3a-C3aR1 signaling is also involved in macrophage-mediated inflammation (25). Alternatively activated macrophages and eosinophils have also been shown to enhance adipocyte browning and protect against diet-induced insulin resistance (41, 42). Therefore, it would be of future interest to determine whether C3a-C3aR1 signaling is involved in macrophage-related adipocyte browning in adipose tissues. Similarly, a study utilizing whole body C3aR1 and C5aR1 single and double KO mice reported increased adipose browning in male receptor KO mice (43). The postulated mechanism involved regulatory T cells and browning via the inosine/A2aR pathway. However, the authors only utilized male mice with general results of adipose browning consistent with this study. Clinical studies have demonstrated sex differences in alternative complement activity and complement component levels in healthy Caucasians (30). Alternative pathway activity is higher in males than in females (30). Circulating levels of C3 are higher in males, while adipsin levels are higher in females (30). Other clinical studies have also confirmed that C3 has higher expression in the cerebrospinal fluid and plasma of men than in women (31, 44). Our results show for the first time that in C57BL/6J mice, circulating levels of adipsin do not differ by sex, but its gene expression is higher in white adipose tissue and thermogenic adipocytes in males than in females. These results suggest that biological sex should be taken into account in alternative complement-related pathology as well as in complement-targeted therapies. Both genetics (such as the X chromosome) and hormonal differences are known to explain the effects of sexual

dimorphism on immunity. But what is causing the difference in the key complement components in the alternative pathway is still unclear. Several clues have suggested that sex may form a possible confounding factor in complement-mediated diseases. For example, in one age-related macular degeneration study, significant differences in alternative pathway component levels were found between the sexes (45). Therefore, further research is needed to elucidate the importance of sexual dimorphism on the complement system. In the future, it will be critical to demonstrate how sex hormones affect the complement system by administrating estrogen and testosterone to healthy and castrated mice of both sexes. Alternative complement levels and activity can also be studied in human study participants receiving hormone replacement therapy.

Although complement factors are best known for treating autoimmune diseases, their effects on adipose thermogenesis are new to the adipose metabolism field. Our analysis reveals that adipocyte-specific knockout of *C3aR1* mice results in major sex differences in response to cold stimulation. In particular, female mice with *C3aR1* KO in adipocytes exhibit pronounced cold intolerance. We do not yet have a mechanistic understanding of the downstream signaling pathway of C3aR1 in regulating the thermogenic gene program in adipocytes and why the results are discrepant between males and females. This may include differences in mitochondrial mass or activity and/or sensitivity to acute and chronic thermogenic stimuli. To our knowledge, this is the first demonstration of sexual dimorphism for brown and beige adipocytes where a molecular receptor shows diametrically opposed functions between sexes. Previous studies have also found sexual dimorphism in the effects of adipose thermogenesis or thermogenesis-related markers (40, 46). Filatov et al. (46) found that the thermogenic protein UCP1 was

induced by cold exposure at the mRNA and protein levels in male Pacap-null mice; however, UCP1 protein induction was attenuated after cold adaptation in female Pacap-null mice. The observed sex-specific differences in the effects of C3aR1 on fat thermogenesis may be related to estrogen. There is evidence for sexual dimorphism in regulation of brown adipose tissue function and adipose tissue browning in rodent models and humans (47, 48). For example, Benz et al. demonstrated that estrogen receptor α signaling in adipocytes can directly activate lipolysis (49). In future studies, it will be of interest to determine if adipocyte C3aR1 is involved in estrogen receptor α signaling-related lipolysis in adipocytes. The mechanistic relationship between estrogen and complement factors remains to be understood with potential for crosstalk between the pathways. Our study highlights that the physiological response to cold stress is regulated differently between the sexes and stresses the importance of analyzing both sexes when assessing mechanisms of energy homeostasis and adaptive thermogenesis in fat.

Methods

Sex as a biological variable

Our study examined male and female animals, and sex-dimorphic effects are reported.

Mice

WT and *Adipsin*$^{-/-}$ mice were backcrossed to C57BL/6J background as described previously (21). Whole body C3aR1 KO mice were purchased from Jackson laboratories (Strain #005712). *C3ar1* floxed mice are on the C57Bl/6J background as described (50). Adipoq-Cre mice were purchased from Jackson laboratories (Strain #028020). *C3ar1* floxed homozygous mice were used in the experiments as controls from the same backcross generation. All mice were maintained in plastic cages under a 12/12-h light/dark cycle at constant temperature (22°C) with free access to water and food. For the diet-induced obesity model, mice were fed a 60% HFD (D12492i, Research Diets) for 16 weeks.

Cold-induced thermogenesis

All the experimental mice were placed in a cold chamber (4°C) for 6 hours (acute cold exposure) or 1 week (chronic cold exposure) with free access to water and food. During acute cold exposure, rectal body temperature was measured using a BAT-12 Microprobe Thermometer (Physitemp, NJ, USA).

Indirect calorimetry

Metabolic rate was measured by indirect calorimetry in metabolic cage, a component of the Comprehensive Lab Animal Monitoring System (CLAMS; Columbus Instruments). Mice were housed individually and maintained at 22°C under a 12/12-h light/dark cycle. Food and water were available ad libitum.

Histological analysis

The adipose tissue was immediately perfused with PBS and fixed with 10% neutral-buffered formalin (VWR). Adipose tissues were then transferred to 70% ethanol. Paraffin embedding, sectioning and the hematoxylin and eosin (H&E) staining were done by the MSKCC Zuckerman Research Center Laboratory of Comparative Pathology core facility. For UCP1 immunohistochemistry, slides were dewaxed in xylene, hydrated in 100%, 95%, 80% and 70% ethanol, and rinsed in water, and antigen retrieval was performed in 10 mM sodium citrate buffer (pH=6.0) by boiling sections. Quenching of endogenous peroxidases was performed using 3% H_2O_2 solution (VWR). Slides were incubated with rabbit polyclonal UCP1 antibody (Abcam, ab10983) overnight at 4°C. Slides were washed in PBST and followed by incubation with HRP-conjugated secondary antibody (goat anti-rabbit, VWR/Jackson Immunoresearch). Then avidin–biotin peroxidase complex (Vectastain ABC kit, PK-7200, Vector Laboratories) was added for 30 min. Slides were developed using 3,3'-diaminobenzidine or 3-amino-9-ethyl carbazole (Sigma) and counterstained with hematoxylin.

In vitro differentiation of primary adipocytes

For primary adipocytes, SVF from inguinal or visceral adipose from 6- to 7-week- old mice was prepared and differentiated for 6–8 days. Primary white adipocytes were cultured in DMEM/F12K media (Gibco) with 10% fetal bovine serum (FBS) at 37C°C, 5% CO2, until confluent. White adipocytes were differentiated via a 48 hours treatment with 0.5 mM 3-isobutyl-1-methylxanthine (IBMX), 1 mM dexamethasone, 850 nM insulin and 1 mM rosiglitazone, followed by 48 hours with 850 nM insulin and 1 mM rosiglitazone, and a further 48 hours with 850 nM insulin. Primary brown adipocytes were cultured in

DMEM/F12K (Gibco) with 10% FBS at 37C°C, 5% CO_2, until confluent. Brown adipocytes were differentiated via a 48 hours treatment with 0.5 mM IBMX, 5 μM dexamethasone,1 nM T3, 2 μM tamoxifen, 400 nM insulin and 1 μM rosiglitazone, followed by 48 hours with 400 nM insulin and 1 μM rosiglitazone, and a further 48 hours with 400 nM insulin. The fully differentiated adipocytes were treated with isoproterenol (10 or 100 nM) for 6 hours.

Seahorse assay

Primary subcutaneous adipocytes and brown adipocytes were plated into 96 well cell culture microplates (Agilent) and cells were plated in seahorse XF base medium (Agilent) containing 2mM L-glutamine and 5mM glucose adjusted to pH7.4. The seahorse microplate was incubated without supplemental CO_2 at 37°C for 1 hour before assay. Oxygen consumption rates and extracellular acidification rates were measured using a XFe96 Seahorse (Agilent Technologies, Santa Clara, CA, USA). 0.5 μM rotenone and antimycin, 1 μM isoproterenol, 3 μM oligomycin and 2 μM carbonyl cyanide 4-(trifluoromethoxy)phenylhydrazone (FCCP) were injected during the assay.

RNA extraction and real-time quantitative PCR

Total RNA from adipose and adipocytes were isolated using the RNeasy Mini kit (Qiagen) per manufacturer's protocol. 1 μg RNA was reverse transcribed using high-capacity cDNA RT kit (Thermo). qPCR was performed using the SYBR Green Master Mix (Quanta) and specific gene primers on QuantStudio 6 Flex system (Thermo Fisher Scientific). Relative mRNA levels were determined by normalized to Ribosomal Protein S18 (Rps18) levels using the Delta-delta-cycle threshold ($\Delta\Delta C_T$) method. Primer sequences are listed in Supplemental Table 1. Approximate C_T values for certain genes are listed in Supplemental Table 2.

Western blot

Adipose tissues were homogenized in in radioimmunoprecipitation assay (RIPA) buffer with protease and phosphatase inhibitor cocktail. Clarified protein extracts were obtained by multiple centrifugation steps and protein concentration measured using Bicinchoninic acid (BCA) assay. Protein extracts were resolved on a NuPAGE Bis-Tris (ThermoFisher) gel and transferred to a PVDF membrane. Membranes were incubated overnight at 4 °C with appropriate primary antibodies. Anti-UCP1 was from Abcam (ab10983) and Anti-beta-actin was from ThermoFisher scientific (MA515739HRP). Detection of proteins was carried out by incubations with horseradish peroxidase (HRP)-conjugated secondary antibodies followed by enhanced chemiluminescence detection reagents. Band density was quantified using Fiji/ImageJ (NIH).

Serum adipsin measurements

For measuring mouse serum adipsin levels, blood was collected from the tail vein, the serum was separated by centrifugation and then adipsin levels were measured by ELISA (R&D) following the manufacturer's protocol.

Isothermal microcalorimeter assay

For heat detection experiments, we used the Cal-ScreenerTM a 48-channel isothermal microcalorimeter (Symcel SverigeAB, Spånga, Sweden), with its corresponding 48-well plate (calPlateTM). Each well consists of a screw-capped titanium vial. Data was continuously collected with the corresponding calViewTM software (Version 1.0.33.0, 2016, Symcel Sverige AB). For the assays, the machine was set and calibrated at 37°C. General handling and device manipulation were done according to the manufacturer's recommendations. We added 400 µL DMEM/F12K media (Gibco) with 10% fetal bovine

serum and around 30-40 mg adipose tissue in each vial. The calView software was used for the calScreener isothermal microcalorimetry (IMC) data collection and analysis. The direct measurement in IMC is heat flow (power in J/s) as a function of time. The heatflow gives the kinetic behavior and response of the sample over time. Data can also be expressed as the total accumulated heat (energy expressed in J) over time as an alternative data presentation of the cellular response to treatment.

Statistics

All statistical analyses were performed using GraphPad Prism9. Unpaired two-tailed Student's t tests and two-way ANOVA were used. $p < 0.05$ was considered statistically significant.

Study approval

All animal studies were approved by the Institutional Animal Care and Use Committee and Research Animal Resource Center at Weill Cornell Medical College.

Data availability

The main data supporting the findings of this study are available within the article and its supplemental files, including the Supporting Data Values. Additional data are available from the corresponding author upon reasonable request.

Author Contributions

L.M. and J.C.L. designed the study and wrote the manuscript with input from all authors. L.M., A.G., A.R.N., E.C.A., S.M.R. and A.L. performed and analyzed the animal experiments. L.M., A.G., and A.R.N. developed and analyzed the in vitro experiments. S.M.R. and L.T. provided scientific input. J.C.L. conceived and supervised the study.

Acknowledgments

We thank Dr. Peter S. Heeger from Cedars-Sinai for generously providing the *C3ar1* floxed mice. We thank Dr. Bruce M. Spiegelman from Harvard for his advice on the project. L.M. was supported by a CSC Scholarship (201906050127). A.G. is supported by an ADA postdoctoral fellowship. J.C.L. is supported by NIH R01 DK121140, R01 DK121844, and R01 DK132879. This work was also supported by R01 DK126944 (S.M.R.). The views expressed in this manuscript are those of the authors and do not necessarily represent the official views of the National Institute of Diabetes and Digestive and Kidney Diseases or the National Institutes of Health. Graphical abstract was created with Biorender.com.

References

1. Powell-Wiley TM, Poirier P, Burke LE, Despres JP, Gordon-Larsen P, Lavie CJ, et al. Obesity and Cardiovascular Disease: A Scientific Statement From the American Heart Association. *Circulation.* 2021;143(21):e984-e1010.
2. Gonzalez-Muniesa P, Martinez-Gonzalez MA, Hu FB, Despres JP, Matsuzawa Y, Loos RJF, et al. Obesity. *Nat Rev Dis Primers.* 2017;3:17034.
3. Yanovski SZ, and Yanovski JA. Long-term drug treatment for obesity: a systematic and clinical review. *JAMA.* 2014;311(1):74-86.
4. Rosenstock J, Wysham C, Frias JP, Kaneko S, Lee CJ, Fernandez Lando L, et al. Efficacy and safety of a novel dual GIP and GLP-1 receptor agonist tirzepatide in patients with type 2 diabetes (SURPASS-1): a double-blind, randomised, phase 3 trial. *Lancet.* 2021;398(10295):143-55.
5. Rizvi AA, and Rizzo M. The Emerging Role of Dual GLP-1 and GIP Receptor Agonists in Glycemic Management and Cardiovascular Risk Reduction. *Diabetes Metab Syndr Obes.* 2022;15:1023-30.
6. Chouchani ET, Kazak L, and Spiegelman BM. New Advances in Adaptive Thermogenesis: UCP1 and Beyond. *Cell Metab.* 2019;29(1):27-37.
7. Cannon B, and Nedergaard J. Brown adipose tissue: function and physiological significance. *Physiol Rev.* 2004;84(1):277-359.
8. Cypess AM, White AP, Vernochet C, Schulz TJ, Xue R, Sass CA, et al. Anatomical localization, gene expression profiling and functional characterization of adult human neck brown fat. *Nat Med.* 2013;19(5):635-9.

9. Cohen P, and Kajimura S. The cellular and functional complexity of thermogenic fat. *Nat Rev Mol Cell Biol.* 2021;22(6):393-409.

10. Wu J, Bostrom P, Sparks LM, Ye L, Choi JH, Giang AH, et al. Beige adipocytes are a distinct type of thermogenic fat cell in mouse and human. *Cell.* 2012;150(2):366-76.

11. Lee YH, Petkova AP, Konkar AA, and Granneman JG. Cellular origins of cold-induced brown adipocytes in adult mice. *FASEB J.* 2015;29(1):286-99.

12. Long JZ, Svensson KJ, Tsai L, Zeng X, Roh HC, Kong X, et al. A smooth muscle-like origin for beige adipocytes. *Cell Metab.* 2014;19(5):810-20.

13. Pollard AE, and Carling D. Thermogenic adipocytes: lineage, function and therapeutic potential. *Biochem J.* 2020;477(11):2071-93.

14. Shao M, Wang QA, Song A, Vishvanath L, Busbuso NC, Scherer PE, et al. Cellular Origins of Beige Fat Cells Revisited. *Diabetes.* 2019;68(10):1874-85.

15. Sakers A, De Siqueira MK, Seale P, and Villanueva CJ. Adipose-tissue plasticity in health and disease. *Cell.* 2022;185(3):419-46.

16. Cypess AM, Lehman S, Williams G, Tal I, Rodman D, Goldfine AB, et al. Identification and importance of brown adipose tissue in adult humans. *N Engl J Med.* 2009;360(15):1509-17.

17. van Marken Lichtenbelt WD, Vanhommerig JW, Smulders NM, Drossaerts JM, Kemerink GJ, Bouvy ND, et al. Cold-activated brown adipose tissue in healthy men. *N Engl J Med.* 2009;360(15):1500-8.

18. Virtanen KA, Lidell ME, Orava J, Heglind M, Westergren R, Niemi T, et al. Functional brown adipose tissue in healthy adults. *N Engl J Med.* 2009;360(15):1518-25.

19. Dunkelberger JR, and Song WC. Complement and its role in innate and adaptive immune responses. *Cell Res.* 2010;20(1):34-50.

20. Mamane Y, Chung Chan C, Lavallee G, Morin N, Xu LJ, Huang J, et al. The C3a anaphylatoxin receptor is a key mediator of insulin resistance and functions by modulating adipose tissue macrophage infiltration and activation. *Diabetes.* 2009;58(9):2006-17.

21. Lo JC, Ljubicic S, Leibiger B, Kern M, Leibiger IB, Moede T, et al. Adipsin is an adipokine that improves beta cell function in diabetes. *Cell.* 2014;158(1):41-53.

22. Shim K, Begum R, Yang C, and Wang H. Complement activation in obesity, insulin resistance, and type 2 diabetes mellitus. *World J Diabetes.* 2020;11(1):1-12.

23. Choy LN, Rosen BS, and Spiegelman BM. Adipsin and an endogenous pathway of complement from adipose cells. *J Biol Chem.* 1992;267(18):12736-41.

24. Gomez-Banoy N, Guseh JS, Li G, Rubio-Navarro A, Chen T, Poirier B, et al. Adipsin preserves beta cells in diabetic mice and associates with protection from type 2 diabetes in humans. *Nat Med.* 2019;25(11):1739-47.

25. Lim J, Iyer A, Suen JY, Seow V, Reid RC, Brown L, et al. C5aR and C3aR antagonists each inhibit diet-induced obesity, metabolic dysfunction, and adipocyte and macrophage signaling. *FASEB J.* 2013;27(2):822-31.

26. Wu J, Cohen P, and Spiegelman BM. Adaptive thermogenesis in adipocytes: Is beige the new brown? *Gene Dev.* 2013;27(3):234-50.

27. Trouw LA, Pickering MC, and Blom AM. The complement system as a potential therapeutic target in rheumatic disease. *Nat Rev Rheumatol.* 2017;13(9).

28. Zwarthoff SA, Berends ETM, Mol S, Ruyken M, Aerts PC, Jozsi M, et al. Functional Characterization of Alternative and Classical Pathway C3/C5 Convertase Activity and Inhibition Using Purified Models. *Frontiers in Immunology.* 2018;9.

29. Mayilyan KR. Complement genetics, deficiencies, and disease associations. *Protein Cell.* 2012;3(7):487-96.

30. Gaya da Costa M, Poppelaars F, van Kooten C, Mollnes TE, Tedesco F, Wurzner R, et al. Age and Sex-Associated Changes of Complement Activity and Complement Levels in a Healthy Caucasian Population. *Front Immunol.* 2018;9:2664.

31. Kamitaki N, Sekar A, Handsaker RE, de Rivera H, Tooley K, Morris DL, et al. Complement genes contribute sex-biased vulnerability in diverse disorders. *Nature.* 2020;582(7813):577-81.

32. Chen Y, Ikeda K, Yoneshiro T, Scaramozza A, Tajima K, Wang Q, et al. Thermal stress induces glycolytic beige fat formation via a myogenic state. *Nature.* 2019;565(7738):180-5.

33. Ikeda K, Kang Q, Yoneshiro T, Camporez JP, Maki H, Homma M, et al. UCP1-independent signaling involving SERCA2b-mediated calcium cycling regulates beige fat thermogenesis and systemic glucose homeostasis. *Nat Med.* 2017;23(12):1454-65.

34. Oeckl J, Janovska P, Adamcova K, Bardova K, Brunner S, Dieckmann S, et al. Loss of UCP1 function augments recruitment of futile lipid cycling for thermogenesis in murine brown fat. *Mol Metab.* 2022;61:101499.

35. Rahbani JF, Bunk J, Lagarde D, Samborska B, Roesler A, Xiao H, et al. Parallel control of cold-triggered adipocyte thermogenesis by UCP1 and CKB. *Cell Metab.* 2024;36(3):526-40 e7.

36. Rahbani JF, Roesler A, Hussain MF, Samborska B, Dykstra CB, Tsai L, et al. Creatine kinase B controls futile creatine cycling in thermogenic fat. *Nature.* 2021;590(7846):480-5.

37. Sun Y, Rahbani JF, Jedrychowski MP, Riley CL, Vidoni S, Bogoslavski D, et al. Mitochondrial TNAP controls thermogenesis by hydrolysis of phosphocreatine. *Nature.* 2021;593(7860):580-5.

38. Pfeifer A, and Hoffmann LS. Brown, beige, and white: the new color code of fat and its pharmacological implications. *Annu Rev Pharmacol Toxicol.* 2015;55:207-27.

39. Forneris F, Ricklin D, Wu J, Tzekou A, Wallace RS, Lambris JD, et al. Structures of C3b in complex with factors B and D give insight into complement convertase formation. *Science.* 2010;330(6012):1816-20.

40. Campbell WD, Lazoura E, Okada N, and Okada H. Inactivation of C3a and C5a octapeptides by carboxypeptidase R and carboxypeptidase N. *Microbiol Immunol.* 2002;46(2):131-4.

41. Molofsky AB, Nussbaum JC, Liang HE, Van Dyken SJ, Cheng LE, Mohapatra A, et al. Innate lymphoid type 2 cells sustain visceral adipose tissue eosinophils and alternatively activated macrophages. *J Exp Med.* 2013;210(3):535-49.

42. Wu D, Molofsky AB, Liang HE, Ricardo-Gonzalez RR, Jouihan HA, Bando JK, et al. Eosinophils sustain adipose alternatively activated macrophages associated with glucose homeostasis. *Science.* 2011;332(6026):243-7.

43. Kong LR, Chen XH, Sun Q, Zhang KY, Xu L, Ding L, et al. Loss of C3a and C5a receptors promotes adipocyte browning and attenuates diet-induced obesity via activating inosine/A2aR pathway. *Cell Rep.* 2023;42(2):112078.

44. Ritchie RF, Palomaki GE, Neveux LM, Navolotskaia O, Ledue TB, and Craig WY. Reference distributions for complement proteins C3 and C4: a practical, simple and clinically relevant approach in a large cohort. *J Clin Lab Anal.* 2004;18(1):1-8.

45. Silva AS, Teixeira AG, Bavia L, Lin F, Velletri R, Belfort R, Jr., et al. Plasma levels of complement proteins from the alternative pathway in patients with age-related macular degeneration are independent of Complement Factor H Tyr(4)(0)(2)His polymorphism. *Mol Vis.* 2012;18:2288-99.

46. Filatov E, Short LI, Forster MAM, Harris SS, Schien EN, Hughes MC, et al. Contribution of thermogenic mechanisms by male and female mice lacking pituitary adenylate cyclase-activating polypeptide in response to cold acclimation. *Am J Physiol Endocrinol Metab.* 2021;320(3):E475-E87.

47. Frank AP, Palmer BF, and Clegg DJ. Do estrogens enhance activation of brown and beiging of adipose tissues? *Physiol Behav.* 2018;187:24-31.

48. Kaikaew K, Grefhorst A, and Visser JA. Sex Differences in Brown Adipose Tissue Function: Sex Hormones, Glucocorticoids, and Their Crosstalk. *Front Endocrinol (Lausanne).* 2021;12:652444.

49. Benz V, Bloch M, Wardat S, Bohm C, Maurer L, Mahmoodzadeh S, et al. Sexual dimorphic regulation of body weight dynamics and adipose tissue lipolysis. *PLoS One.* 2012;7(5):e37794.

50. Cumpelik A, Heja D, Hu Y, Varano G, Ordikhani F, Roberto MP, et al. Dynamic regulation of B cell complement signaling is integral to germinal center responses. *Nat Immunol.* 2021;22(6):757-68.

Figure Legends

Figure 1. Mice deficient in Adipsin are protected from diet-induced obesity and display evidence of enhanced energy expenditure.

A) Body weights of wild type (WT), *Adipsin* heterozygous and knockout (KO) male mice on high fat diet (HFD) for the indicated number of weeks. n = 8-14/group. Unpaired Welch's t-test is used for comparison between WT and KO groups.

B) Body composition of male mice from (A) after 12 weeks of HFD. n = 8-14/group. 2 way ANOVA with Tukey's multiple comparisons was used for comparison between WT, heterozygous, and KO groups.

C) Food intake of male mice from (A) was measured daily after 4 weeks on HFD. n = 7-8/group.

D and **E)** O_2 consumption (**D**) and CO_2 production (**E**) rates of WT and *Adipsin* knockout male mice were measured by indirect calorimetry after 4 weeks on HFD. n= 7-8/group. Unpaired t-test is used for comparison.

Data are presented as mean± S.E.M. *$p < 0.05$.

Figure 2. Adipsin deficiency promotes white adipose beiging.

A and **B)** Thermogenic gene expression in visceral (VISC) (**A**) and subcutaneous (SubQ) (**B**) fat of 10-12 week old WT and *Adipsin* knockout male mice fed a regular diet at ambient temperature. N=4-5/group.

C) Thermogenic gene expression in SubQ fat of 10-12 week old WT and *Adipsin* knockout male mice following an acute (6 hours) cold exposure. N=10-11/group.

D) Hematoxylin and eosin (H&E) and UCP1 immunohistochemistry staining of inguinal white adipose tissue sections from 10 week old WT and *Adipsin* knockout male mice at room temperature (RT) and following acute cold exposure. Images are shown at 20x magnification. Scale bar, 200 μm.

E) Thermogenic gene expression in primary subcutaneous adipocytes treated with or without isoproterenol (Iso) from WT and *Adipsin* knockout mice. n=3/group.

F) Thermogenic gene expression in primary subcutaneous adipocytes treated with or without isoproterenol (Iso) from WT and *C3aR1* knockout mice. n=5-6/group.

Data are presented as mean± S.E.M. Unpaired t-test is used for comparison between WT and KO, and WT + Iso and KO + Iso groups for E and F. *p < 0.05, **p < 0.01, ***p < 0.001.

Figure 3. Adipocyte-specific C3aR1 knockout male mice and adipose thermogenic capacity in vitro and in vivo.

A) *C3aR1* gene expression in the adipocyte fraction of 7 week old control and Ad-*C3aR1*$^{-/-}$ male mice fed a regular diet at ambient temperature. n=2-3/group.

B) Thermogenic gene expression in primary subcutaneous adipocytes treated with isoproterenol (Iso) from control and Ad-*C3aR1*$^{-/-}$ male mice. n=4/group.

C) Oxygen consumption rate (OCR) of primary control and Ad-*C3aR1* knockout subcutaneous adipocytes. ISO: isoproterenol; FCCP: carbonyl cyanide 4 (trifluoromethoxy) phenylhydrazone; Rot: rotenone; Ant: antimycin. n=18-20/group.

D-G) Quantification of isoproterenol-stimulated OCR (**D**), maximal respiratory capacity (**E**), Adenosine triphosphate (ATP)-coupled OCR (**F**), and uncoupled OCR (**G**) from primary control and Ad-*C3aR1* knockout subcutaneous adipocytes.

H) Thermogenic gene expression in subcutaneous (SubQ) fat of 10-12 week old control and Ad-*C3aR1*$^{-/-}$ male mice fed a regular diet at ambient temperature. n=7/group.

I) Body temperature of 10-12 week old control and Ad-*C3aR1*$^{-/-}$ male mice during acute cold exposure. n=7-10/group.

Data are presented as mean± S.E.M. Unpaired two-tailed t test is used for comparison. *p < 0.05, **p < 0.01, ***p < 0.001.

Figure 4. Sex-dependent differences in alternative complement pathway components.

A) ELISA for adipsin from serum of male and female wild type (WT) mice at 10-11 week old on regular diet. n=8/group.

B-D) Relative *Adipsin* and *C3aR1* gene expression in subcutaneous (SubQ) (**B**), visceral (VISC) (**C**) and brown (**D**) adipose tissue of 10-11 week old male and female WT mice on regular diet. n=4-5/group.

E) Relative *Adipsin* gene expression in the adipocyte fraction of 10-11 week old male and female WT mice on regular diet. n=4/group.

Data are presented as mean± S.E.M. Unpaired two-tailed t test is used for comparison. *p < 0.05, **p < 0.01, ***p < 0.001.

Figure 5. Adipocyte-specific *C3aR1* knockout female mice have impaired thermogenic capacity and are cold intolerant.

A) Body temperature of control and Ad-*C3aR1* knockout female mice during acute cold exposure. n=5/group.

B) Thermogenic gene expression in brown adipose tissue (BAT) of 10-12 week old control and Ad-*C3aR1*$^{-/-}$ female mice following an acute (6 hour) cold exposure. n=5-8/group.

C) Brown fat UCP1 protein levels normalized to actin by Western blot in control and Ad-*C3aR1*$^{-/-}$ female mice at ambient temperature**.** n=5/group.

D) Subcutaneous fat UCP1 protein levels normalized to actin by Western blot in control and Ad-*C3aR1*$^{-/-}$ female mice at ambient temperature**.** n=4-5/group.

E) Accumulated heat in J recorded from wells in duplicates containing adipose tissue from control and Ad-*C3aR1*$^{-/-}$ female mice fed a regular diet at ambient temperature. n=4/group. Data are presented as mean± S.E.M. Unpaired two-tailed t test is used for comparison. *$p < 0.05$, **$p < 0.01$.

Supplemental Figure Legends

Supplemental Figure 1.

A) *Adipsin* mRNA expression in adipose tissues of 10-12 week old wild type (WT) and *Adipsin* knockout male mice fed a regular diet at ambient temperature. N=5-6/group.

B) Body weights of WT and *Adipsin* knockout male mice on 12 weeks of regular diet. N=9-11/group.

C and **D)** O_2 consumption (**C**) and CO_2 production (**D**) rates of WT and *Adipsin* knockout male mice were measured by indirect calorimetry after 4 weeks on high fat diet (HFD). N=8/group.

E) Locomotor activity of WT and *Adipsin* knockout male mice after 4 weeks of HFD measured in metabolic chambers. N=8/group.

Data are presented as mean± S.E.M. Unpaired t-test is used for comparison between groups in **A** and **B**. *p < 0.05, **p < 0.01, ***p < 0.001.

Supplemental Figure 2.

A) Thermogenic gene expression in brown adipose tissue (BAT) of 10-12 weeks old wild type (WT) and *Adipsin* knockout male mice fed a regular diet at ambient temperature. N=5/group.

B) Body temperature of 10-12 week old control and Ad-*C3aR1*$^{-/-}$ male and female mice during acute cold exposure. n=10-11/group for males and n=15-18/group for females.

C) Thermogenic gene expression in visceral (VISC) fat of 10-12 weeks old WT and *Adipsin* knockout male mice following an acute (6 hour) cold exposure. n=10-11/group.

D) Thermogenic gene expression in BAT of 10-12 week old WT and *Adipsin* knockout male mice following an acute (6 hour) cold exposure. n=5/group.

E) UCP1-independent thermogenic gene expression in subcutaneous (SubQ) fat of 10-12 week old WT and *Adipsin* knockout male mice following an acute (6 hour) cold exposure. n=8-11/group.

F-H) Thermogenic gene expression in VISC (**F**), SubQ (**G**) and brown (**H**) fat of 10-12 week old WT and *Adipsin* knockout male mice following a chronic (1 week) cold exposure. n=4-5/group.

I-J) O_2 consumption (**I**) and CO_2 production (**J**) rates of WT and *C3ar1* knockout mice were measured by indirect calorimetry after 4 weeks on high fat diet (HFD). n=5/group.

Data are presented as mean± S.E.M. Unpaired two-tailed t test is used for comparison. n.s., not significant. *p < 0.05, **p < 0.01, ***p < 0.001.

Supplemental Figure 3.

A) Thermogenic gene expression in primary brown adipocytes treated with isoproterenol from control and Ad-*C3aR1*$^{-/-}$ male mice. n=4/group.

B) OCR of primary control and Ad-*C3aR1* knockout brown adipocytes. n=20/group.

C-F) Quantification of isoproterenol-stimulated OCR (**C**), maximal respiratory capacity (**D**), Adenosine triphosphate (ATP)-coupled OCR (**E**), and uncoupled OCR (**F**) from primary control and Ad-*C3aR1* knockout brown adipocytes. n=20/group.

G and **H)** Thermogenic gene expression in brown (**G**) and visceral (VISC) (**H**) fat of 10-12 week old control and Ad-*C3aR1* knockout male mice fed a regular diet at ambient temperature. n=4/group.

I) Brown fat UCP1 protein levels normalized to actin by Western blot in control and Ad-*C3aR1*$^{-/-}$ male mice at ambient temperature**.** n=6/group.

J) Subcutaneous fat UCP1 protein levels normalized to actin by Western blot in control and Ad-*C3aR1*$^{-/-}$ male mice at ambient temperature**.** n=5/group.

K) Body weights of control and Ad-*C3aR1* knockout male mice at room temperature and 6 hours post cold exposure. n=7-12/group.

L) Accumulated heat in J recorded from wells in duplicates containing adipose tissue from control and Ad-*C3aR1*$^{-/-}$ male mice fed a regular diet at ambient temperature. n=4/group.

M) Heat flow in mW recorded from wells in duplicates containing adipose tissue from control and Ad-*C3aR1*$^{-/-}$ male mice fed a regular diet at ambient temperature. n=4/group. Data are presented as mean± S.E.M. Unpaired two-tailed t test is used for comparison.

Supplemental Figure 4.

A) Body weight of control and Ad-*C3aR1* knockout female mice at room temperature and 6 hours post cold exposure. n=5/group.

B) Thermogenic gene expression in brown adipose tissue (BAT) of 10-12 week old control and Ad-*C3aR1*$^{-/-}$ female mice at room temperature. n=5-6/group.

C) Thermogenic gene expression of subcutaneous (SubQ) fat in 10-12 weeks WT and Ad-*C3aR1* knockout female mice following an acute (6 hour) cold exposure. n=5-8/group.

D) Heat flow in mW recorded from wells in duplicates containing adipose tissue from control and Ad-*C3aR1*$^{-/-}$ female mice fed a regular diet at ambient temperature. n=4/group.

E and **F)** Hematoxylin and eosin (**E**) and UCP1 (**F**) immunohistochemistry staining of brown adipose tissue (BAT) sections from 10-week-old control and Ad-*C3aR1* knockout

female mice at room temperature (RT) and following acute cold exposure. Representative images are shown at 20x magnification. Scale bar, 200 μm.

G and **H**) Thermogenic gene expression in primary subcutaneous (**G**) and brown (**H**) adipocytes treated with isoproterenol (Iso) from control and Ad-*C3aR1*$^{-/-}$ female mice. n=4/group.

Data are presented as mean± S.E.M. Unpaired two-tailed t test is used for comparison. *p < 0.05, **p < 0.01.

Supplemental Table 1. qPCR primer sequences

Gene	Forward	Reverse
Rps18	CATGCAGAACCCACGACAGTA	CCTCACGCAGCTTGTTGTCTA
C3ar1	TGACAGGTCAGCTCCTTCCT	CATTAGGAGGCTTTCCACCA
Ucp1	ACTGCCACACCTCCAGTCATT	CTTTGCCTCACTCAGGATTGG
Prdm16	CAGCACGGTGAAGCCATTC	GCGTGCATCCGCTTGTG
Ppargc1a	CCCTGCCATTGTTAAGACC	TGCTGCTGTTCCTGTTTTC
Ppargc1b	AGTCAGCGGCCTTGTGTCAA	ACTCTGGGACAGGGCAGCA
Adipsin	CGTACCATGACGGGGTAGTC	ATCCGGTAGGATGACACTCG
Alpl	CCAACTCTTTTGTGCCAGAGA	GGCTACATTGGTGTTGAGCTTTT
Cidea	TGCTCTTCTGTATCGCCCAGT	GCCGTGTTAAGGAATCTGCTG
Dio2	CAGTGTGGTGCACGTCTCCAATC	TGAACCAAAGTTGACCACCAG
Elovl3	TCCGCGTTCTCATGTAGGTCT	GGACCTGATGCAACCCTATGA
Serca1	TCATTGCCAACGCCATTGTG	CAGCCCGATAGACCTTTCCC
Serca2b	ACCTTTGCCGCTCATTTTCCAG	AGGCTGCACACACTCTTTACC
Ryr2	CTTCTGTGAGGACACCATCTTT	CCTCTCCTTCTCACTCTCTTCT
Sdhb	TAGCGGTCCTCAGGGTGAGA	CTGAAACTGCAGGCCGACTCT
Ckb	CTGTCTGGCAGGTACTACGC	TGCATGGAGATGACTCGCAG
Ckm	GAACCTCAAGGGTGGAGACG	GTTGAGAGCTTCCACGGACA
Ckmt1	TGACCCCTATTTTGGCTCCAG	TTGGGGATGCGGCTACAAAG
Ldhb	CAAAGGCTACACCAACTGGG	TTGAGGATGCACGGGAGACT
Pkm	CCTCCAGTCACTCCACAGAC	GCAATGATAGGAGCCCGAGG
Gpr3	ATCTACGCCTTTCGCAACCA	CGGGACCGGAATGGAATCTT
Fabp4	ACACCGAGATTTCCTTCAAACTG	CCATCTAGGGTTATGATGCTCTTCA
Dgat1	GGAGACCGCGAGTTCTACAG	CTCATGGAAGAAGGCTGAGG
Dgat2	TCTCAGCCCTCCAAGACATC	GCCAGCCAGGTGAAGTAGAG

Lpl	GGGAGTTTGGCTCCAGAGTTT	TGTGTCTTCAGGGGTCCTTAG
Gk	ACGGGCCATAAGTGTGTATTT	GAACGAAGTAGCAGCCATAAGA

Supplemental Table 2: C_T values in WT/Control Adipose Tissues at room temperature

Approximate C_T for Gene	Subcutaneous Fat	Brown Fat
Ucp1	23	15
Ckb	-	24
Alpl	-	26
Serca2b	23	21
Ryr2	31	29

C_T for RPS18: ~20

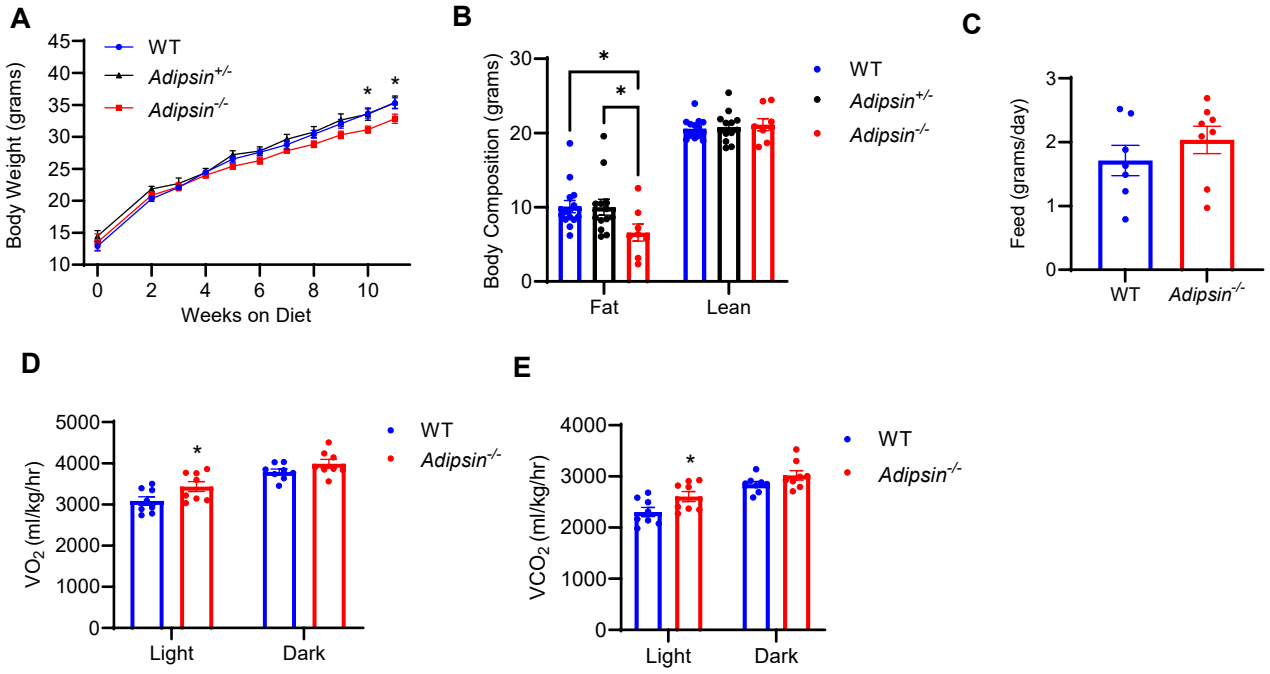

Figure 1. Mice deficient in Adipsin are protected from diet-induced obesity and display evidence of enhanced energy expenditure.
A) Body weights of wild type (WT), *Adipsin* heterozygous and knockout (KO) male mice on high fat diet (HFD) for the indicated number of weeks. n = 8-14/group. Unpaired Welch's t-test is used for comparison between WT and KO groups.
B) Body composition of male mice from (A) after 12 weeks of HFD. n = 8-14/group. 2 way ANOVA with Tukey's multiple comparisons was used for comparison between WT, heterozygous, and KO groups.
C) Food intake of male mice from (A) was measured daily after 4 weeks on HFD. n = 7-8/group.
D and **E)** O_2 consumption (**D**) and CO_2 production (**E**) rates of WT and *Adipsin* knockout male mice were measured by indirect calorimetry after 4 weeks on HFD. n= 7-8/group. Unpaired t-test is used for comparison.
Data are presented as mean± S.E.M. *p < 0.05.

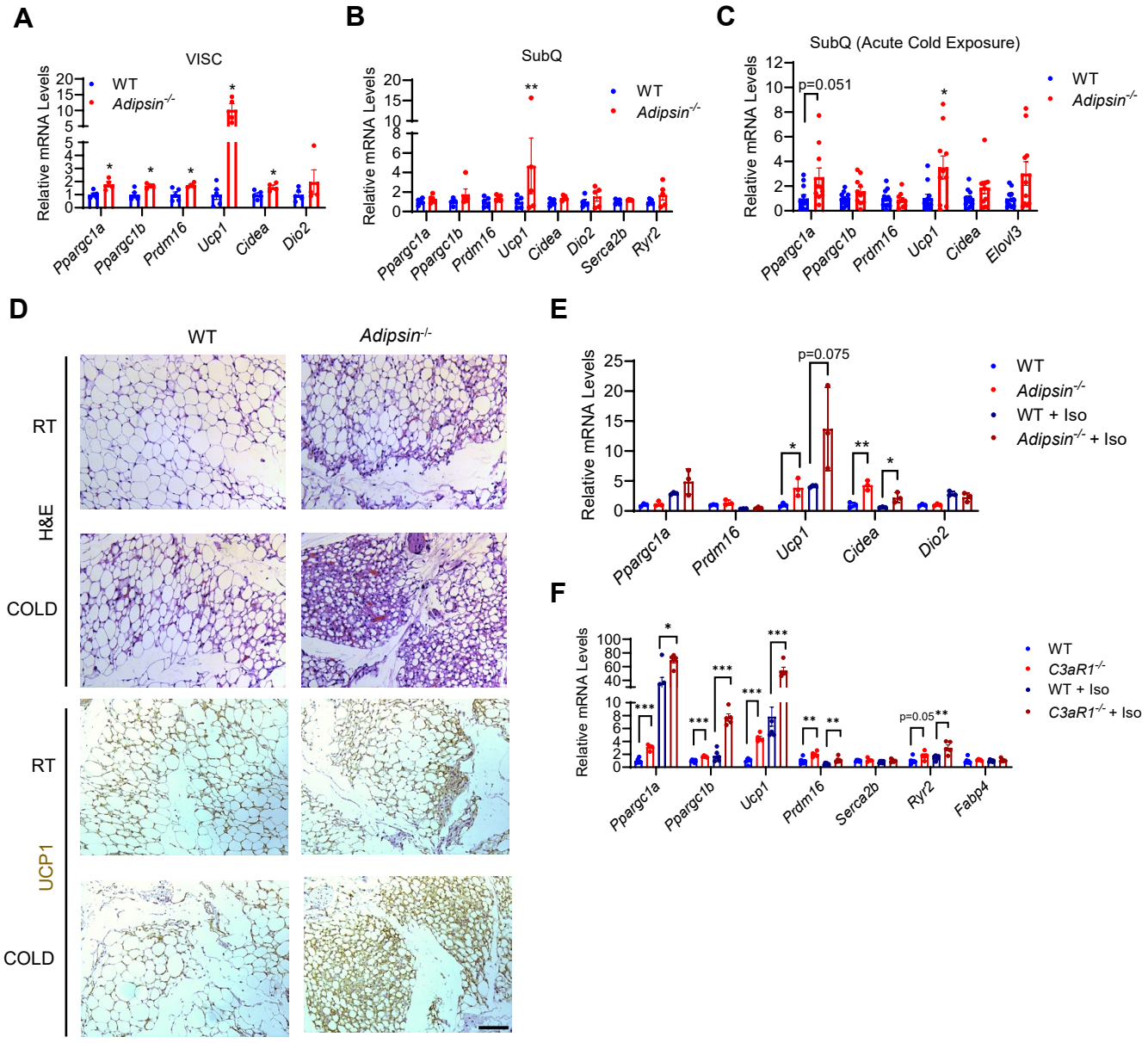

Figure 2. Adipsin deficiency promotes white adipose beiging.

A and **B)** Thermogenic gene expression in visceral (VISC) (**A**) and subcutaneous (SubQ) (**B**) fat of 10-12 week old WT and *Adipsin* knockout male mice fed a regular diet at ambient temperature. N=4-5/group.

C) Thermogenic gene expression in SubQ fat of 10-12 week old WT and *Adipsin* knockout male mice following an acute (6 hours) cold exposure. N=10-11/group.

D) Hematoxylin and eosin (H&E) and UCP1 immunohistochemistry staining of inguinal white adipose tissue sections from 10 week old WT and *Adipsin* knockout male mice at room temperature (RT) and following acute cold exposure. Images are shown at 20x magnification. Scale bar, 200 μm.

E) Thermogenic gene expression in primary subcutaneous adipocytes treated with or without isoproterenol (Iso) from WT and *Adipsin* knockout mice. n=3/group.

F) Thermogenic gene expression in primary subcutaneous adipocytes treated with or without isoproterenol (Iso) from WT and *C3aR1* knockout mice. n=5-6/group.

Data are presented as mean± S.E.M. Unpaired t-test is used for comparison between WT and KO, and WT + Iso and KO + Iso groups for E and F. *p < 0.05, **p < 0.01, ***p < 0.001.

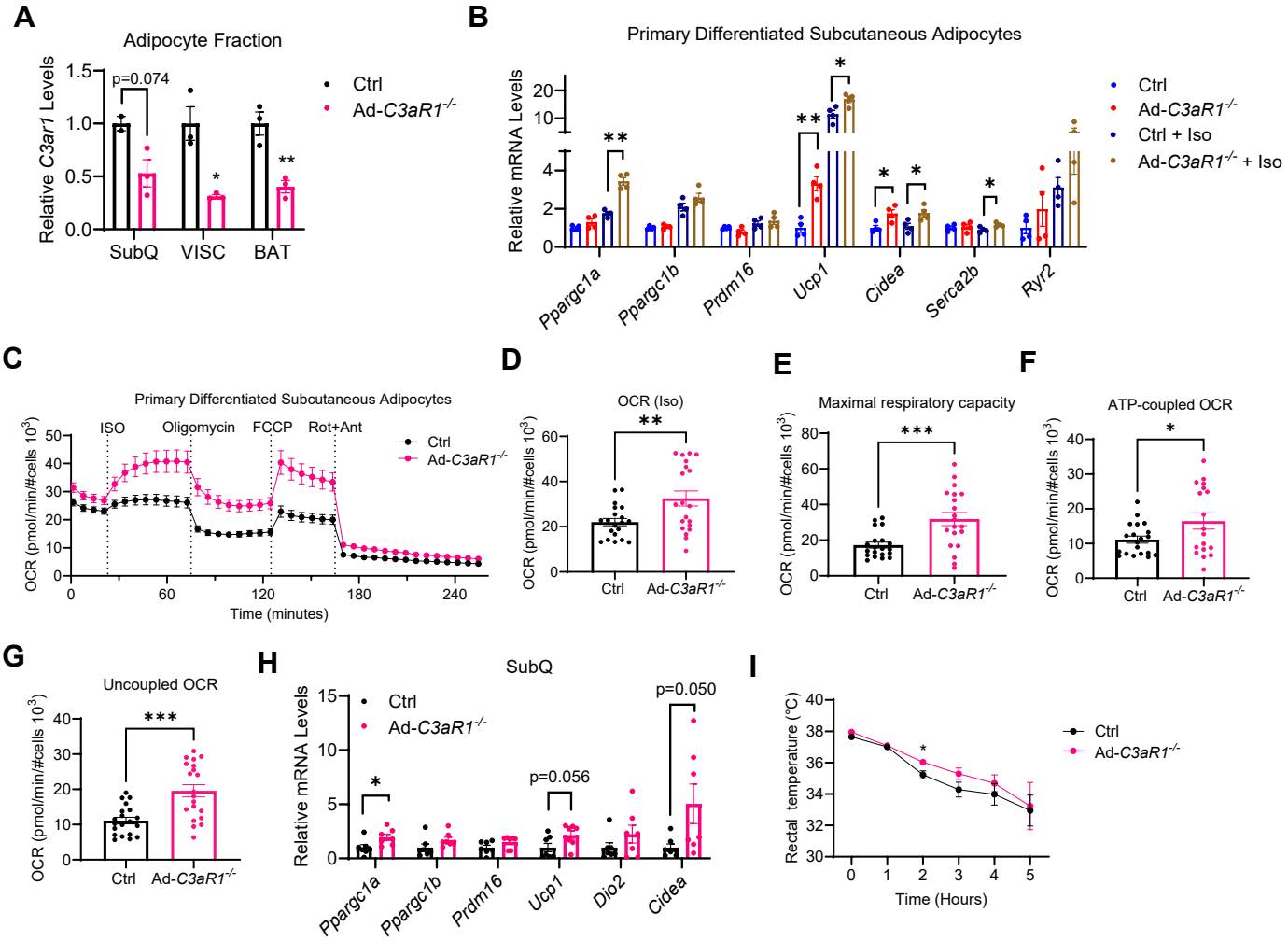

Figure 3. Adipocyte-specific C3aR1 knockout male mice and adipose thermogenic capacity in vitro and in vivo.

A) *C3aR1* gene expression in the adipocyte fraction of 7 week old control and Ad-*C3aR1*$^{-/-}$ male mice fed a regular diet at ambient temperature. n=2-3/group.

B) Thermogenic gene expression in primary subcutaneous adipocytes treated with isoproterenol (Iso) from control and Ad-*C3aR1*$^{-/-}$ male mice. n=4/group.

C) Oxygen consumption rate (OCR) of primary control and Ad-*C3aR1* knockout subcutaneous adipocytes. ISO: isoproterenol; FCCP: carbonyl cyanide 4 (trifluoromethoxy) phenylhydrazone; Rot: rotenone; Ant: antimycin. n=18-20/group.

D-G) Quantification of isoproterenol-stimulated OCR (**D**), maximal respiratory capacity (**E**), Adenosine triphosphate (ATP)-coupled OCR (**F**), and uncoupled OCR (**G**) from primary control and Ad-*C3aR1* knockout subcutaneous adipocytes.

H) Thermogenic gene expression in subcutaneous (SubQ) fat of 10-12 week old control and Ad-*C3aR1*$^{-/-}$ male mice fed a regular diet at ambient temperature. n=7/group.

I) Body temperature of 10-12 week old control and Ad-*C3aR1*$^{-/-}$ male mice during acute cold exposure. n=7-10/group.

Data are presented as mean± S.E.M. Unpaired two-tailed t test is used for comparison. *p < 0.05, **p < 0.01, ***p < 0.001.

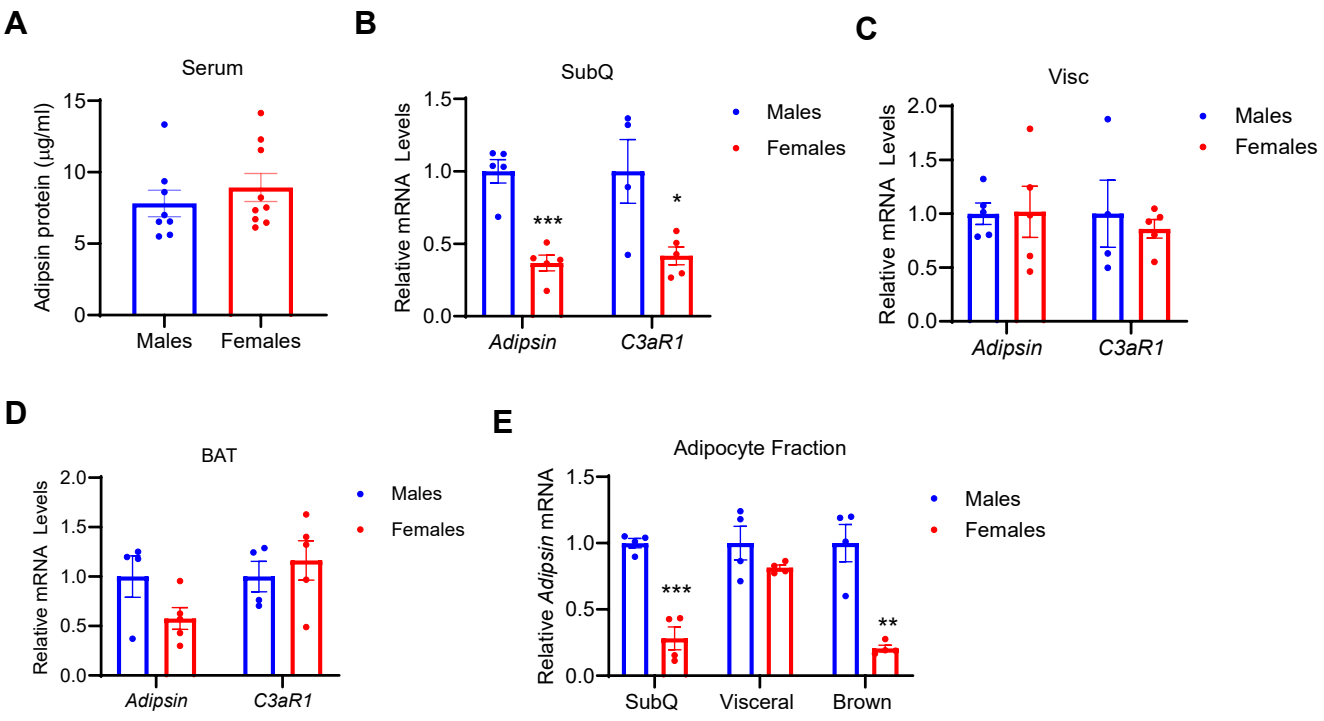

Figure 4. Sex-dependent differences in alternative complement pathway components.
A) ELISA for adipsin from serum of male and female wild type (WT) mice at 10-11 week old on regular diet. n=8/group.
B-D) Relative *Adipsin* and *C3aR1* gene expression in subcutaneous (SubQ) (**B**), visceral (VISC) (**C**) and brown (**D**) adipose tissue of 10-11 week old male and female WT mice on regular diet. n=4-5/group.
E) Relative *Adipsin* gene expression in the adipocyte fraction of 10-11 week old male and female WT mice on regular diet. n=4/group.
Data are presented as mean± S.E.M. Unpaired two-tailed t test is used for comparison. *p < 0.05, **p < 0.01, ***p < 0.001.

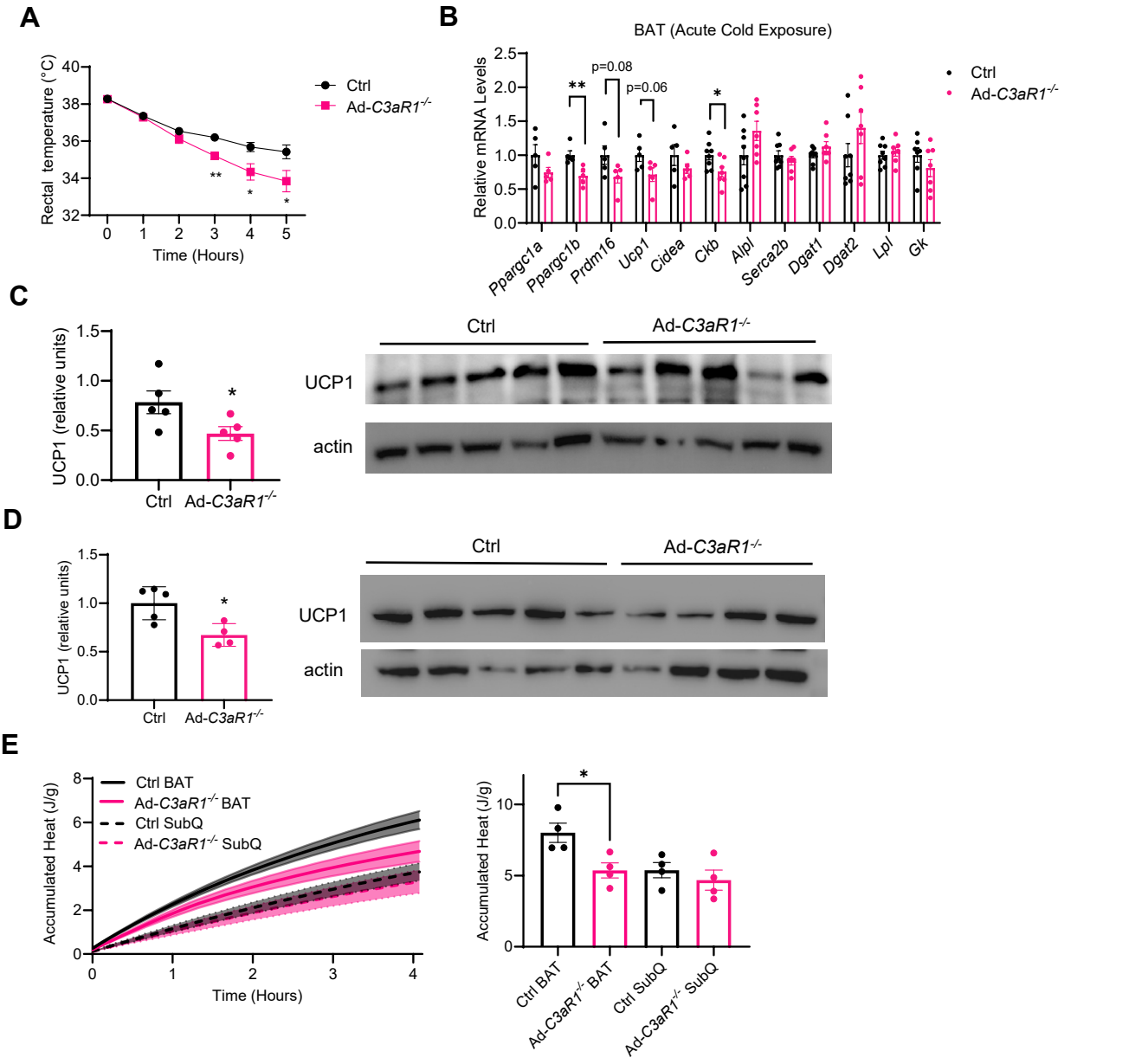

Figure 5. Adipocyte-specific *C3aR1* knockout female mice have impaired thermogenic capacity and are cold intolerant.

A) Body temperature of control and Ad-*C3aR1* knockout female mice during acute cold exposure. n=5/group.

B) Thermogenic gene expression in brown adipose tissue (BAT) of 10-12 week old control and Ad-*C3aR1*$^{-/-}$ female mice following an acute (6 hour) cold exposure. n=5-8/group.

C) Brown fat UCP1 protein levels normalized to actin by Western blot in control and Ad-*C3aR1*$^{-/-}$ female mice at ambient temperature**.** n=5/group.

D) Subcutaneous fat UCP1 protein levels normalized to actin by Western blot in control and Ad-*C3aR1*$^{-/-}$ female mice at ambient temperature**.** n=4-5/group.

E) Accumulated heat in J recorded from wells in duplicates containing adipose tissue from control and Ad-*C3aR1*$^{-/-}$ female mice fed a regular diet at ambient temperature. n=4/group.

Data are presented as mean± S.E.M. Unpaired two-tailed t test is used for comparison. *p < 0.05, **p < 0.01.

SUPPLEMENTAL FIGURES

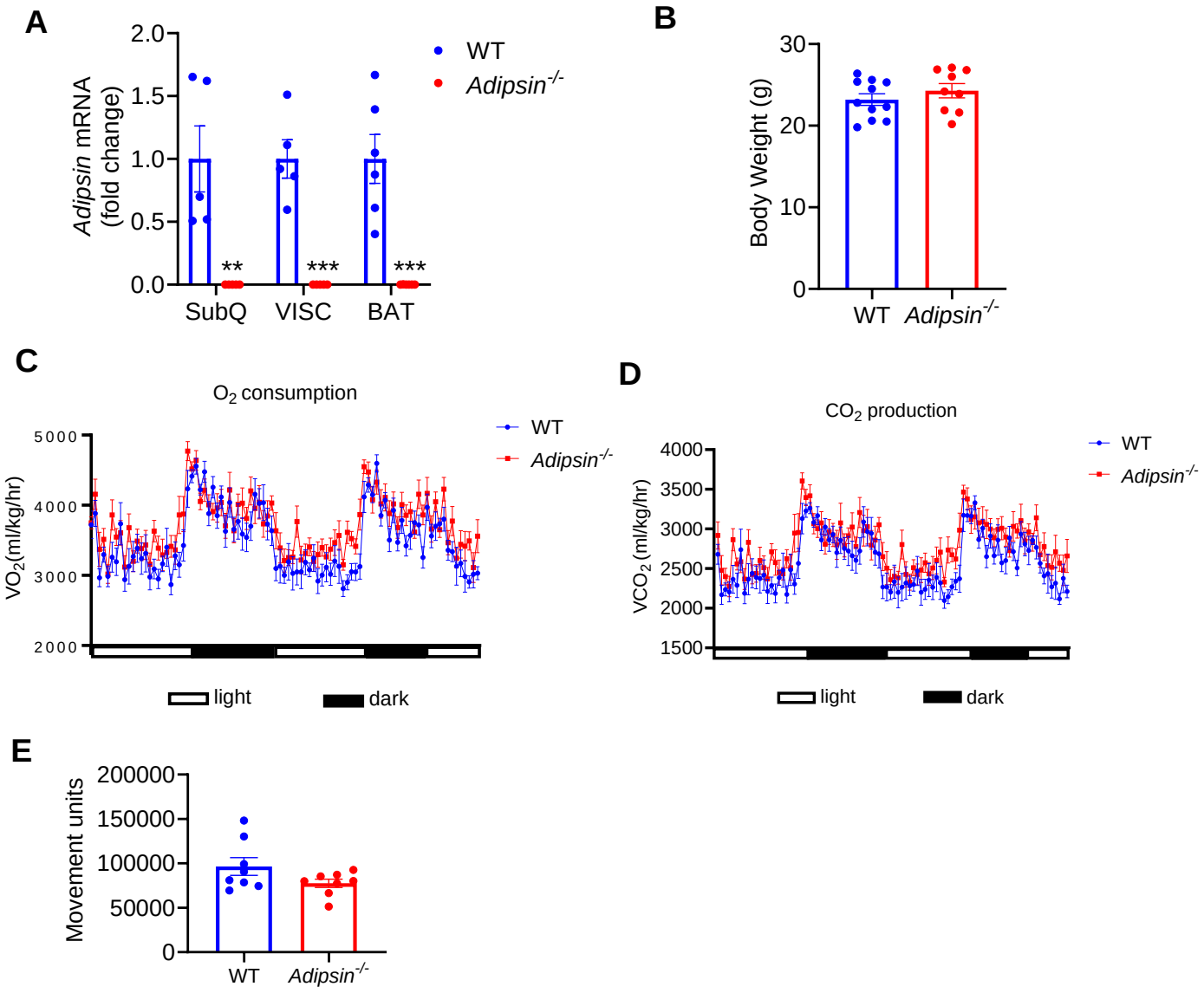

Supplemental Figure 1.

A) *Adipsin* mRNA expression in adipose tissues of 10-12 week old wild type (WT) and *Adipsin* knockout male mice fed a regular diet at ambient temperature. N=5-6/group.

B) Body weights of WT and *Adipsin* knockout male mice on 12 weeks of regular diet. N=9-11/group.

C and **D)** O_2 consumption (**C**) and CO_2 production (**D**) rates of WT and *Adipsin* knockout male mice were measured by indirect calorimetry after 4 weeks on high fat diet (HFD). N=8/group.

E) Locomotor activity of WT and *Adipsin* knockout male mice after 4 weeks of HFD measured in metabolic chambers. N=8/group.

Data are presented as mean± S.E.M. Unpaired t-test is used for comparison between groups in **A** and **B**. *p < 0.05, **p < 0.01, ***p < 0.001.

Supplemental Figure 2

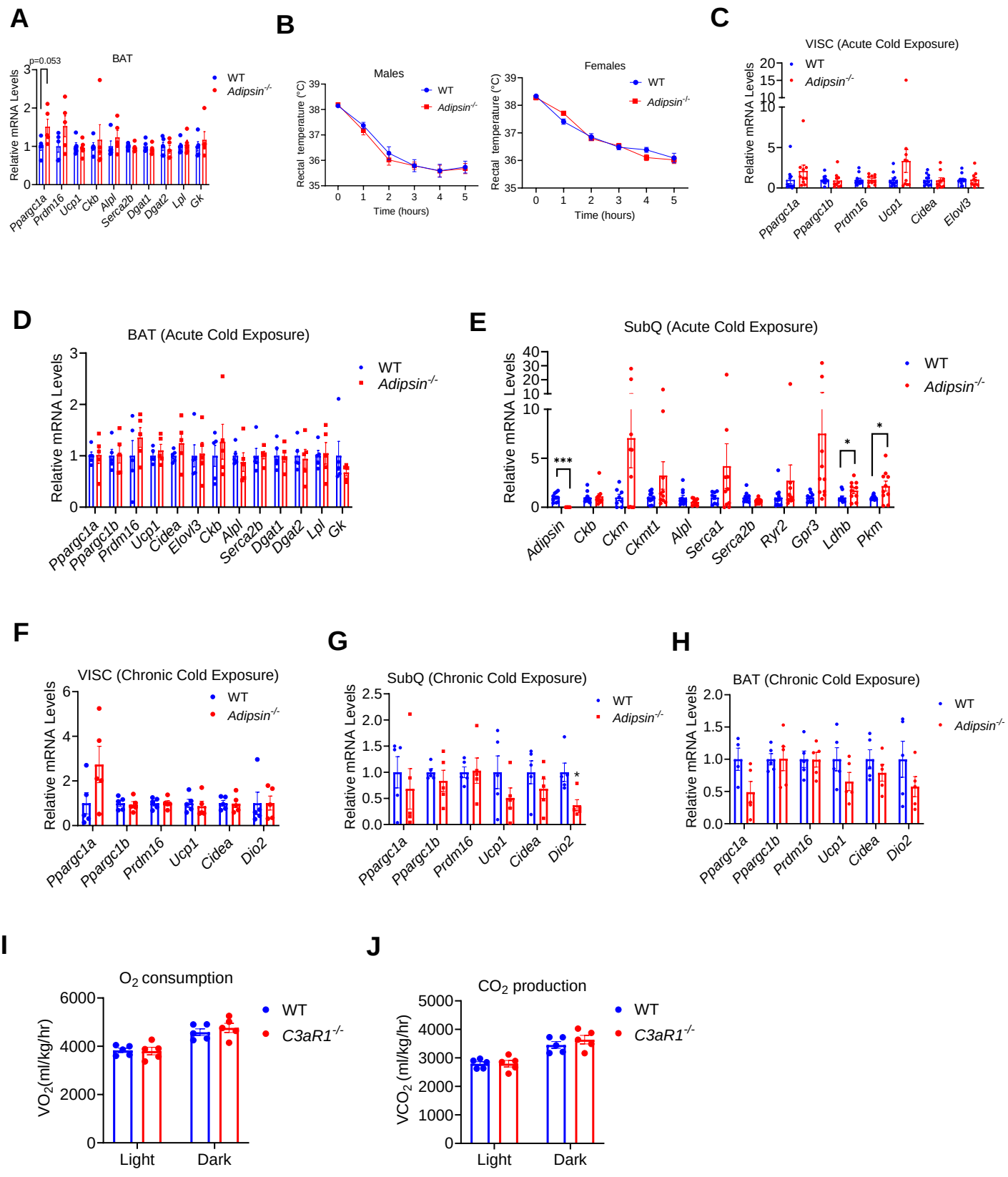

Supplemental Figure 2.

A) Thermogenic gene expression in brown adipose tissue (BAT) of 10-12 weeks old wild type (WT) and *Adipsin* knockout male mice fed a regular diet at ambient temperature. N=5/group.

B) Body temperature of 10-12 week old control and Ad-*C3aR1*$^{-/-}$ male and female mice during acute cold exposure. n=10-11/group for males and n=15-18/group for females.

C) Thermogenic gene expression in visceral (VISC) fat of 10-12 weeks old WT and *Adipsin* knockout male mice following an acute (6 hour) cold exposure. n=10-11/group.

D) Thermogenic gene expression in BAT of 10-12 week old WT and *Adipsin* knockout male mice following an acute (6 hour) cold exposure. n=5/group.

E) UCP1-independent thermogenic gene expression in subcutaneous (SubQ) fat of 10-12 week old WT and *Adipsin* knockout male mice following an acute (6 hour) cold exposure. n=8-11/group.

F-H) Thermogenic gene expression in VISC (**F**), SubQ (**G**) and brown (**H**) fat of 10-12 week old WT and *Adipsin* knockout male mice following a chronic (1 week) cold exposure. n=4-5/group.

I-J) O_2 consumption (**I**) and CO_2 production (**J**) rates of WT and *C3ar1* knockout mice were measured by indirect calorimetry after 4 weeks on high fat diet (HFD). n=5/group.

Data are presented as mean± S.E.M. Unpaired two-tailed t test is used for comparison. n.s., not significant. *p < 0.05, **p < 0.01, ***p < 0.001.

Supplemental Figure 3

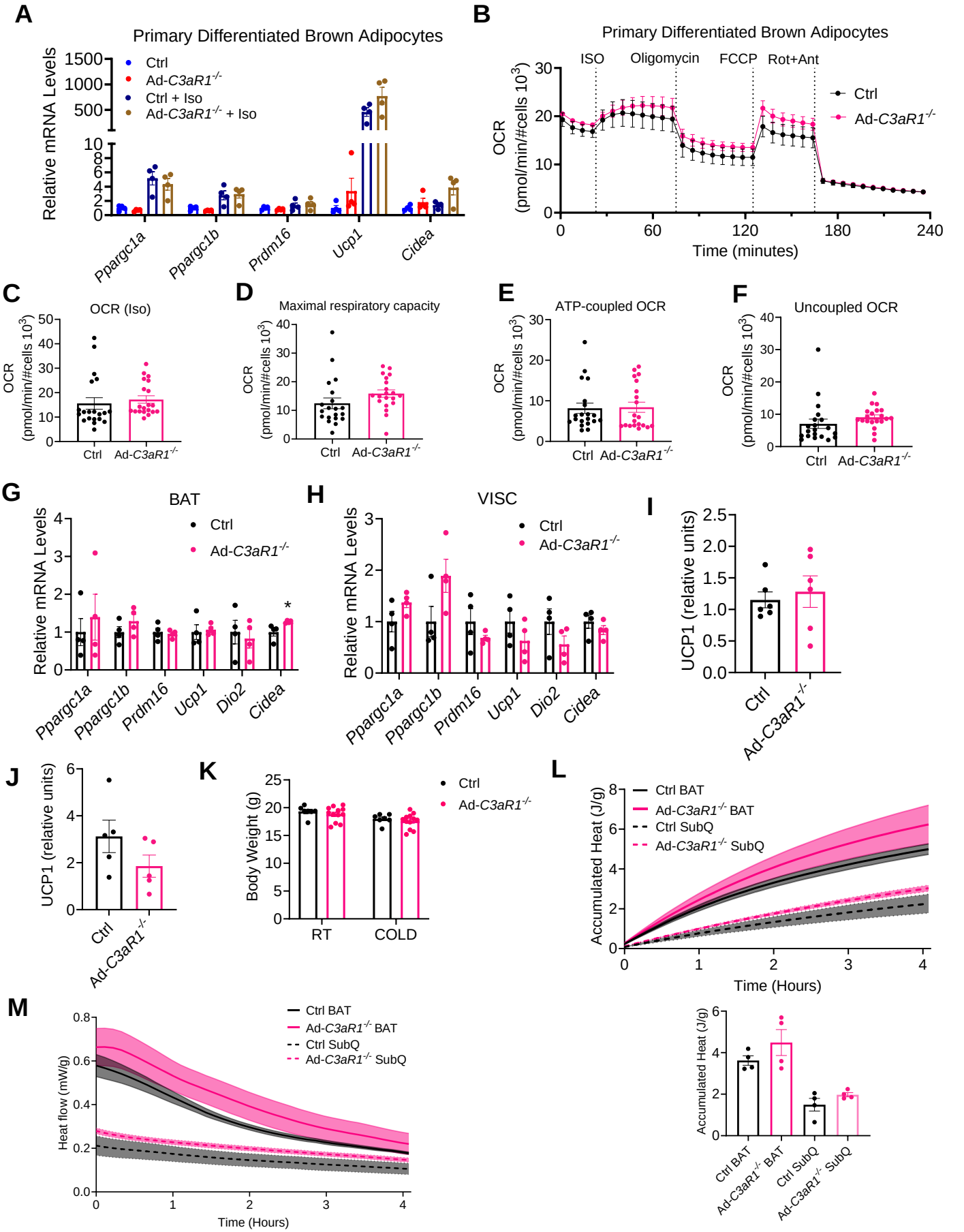

Supplemental Figure 3.

A) Thermogenic gene expression in primary brown adipocytes treated with isoproterenol from control and Ad-*C3aR1*$^{-/-}$ male mice. n=4/group.

B) OCR of primary control and Ad-*C3aR1* knockout brown adipocytes. n=20/group.

C-F) Quantification of isoproterenol-stimulated OCR (**C**), maximal respiratory capacity (**D**), Adenosine triphosphate (ATP)-coupled OCR (**E**), and uncoupled OCR (**F**) from primary control and Ad-*C3aR1* knockout brown adipocytes. n=20/group.

G and **H)** Thermogenic gene expression in brown (**G**) and visceral (VISC) (**H**) fat of 10-12 week old control and Ad-*C3aR1* knockout male mice fed a regular diet at ambient temperature. n=4/group.

I) Brown fat UCP1 protein levels normalized to actin by Western blot in control and Ad-*C3aR1*$^{-/-}$ male mice at ambient temperature**.** n=6/group.

J) Subcutaneous fat UCP1 protein levels normalized to actin by Western blot in control and Ad-*C3aR1*$^{-/-}$ male mice at ambient temperature**.** n=5/group.

K) Body weights of control and Ad-*C3aR1* knockout male mice at room temperature and 6 hours post cold exposure. n=7-12/group.

L) Accumulated heat in J recorded from wells in duplicates containing adipose tissue from control and Ad-*C3aR1*$^{-/-}$ male mice fed a regular diet at ambient temperature. n=4/group.

M) Heat flow in mW recorded from wells in duplicates containing adipose tissue from control and Ad-*C3aR1*$^{-/-}$ male mice fed a regular diet at ambient temperature. n=4/group.

Data are presented as mean± S.E.M. Unpaired two-tailed t test is used for comparison.

Supplemental Figure 4

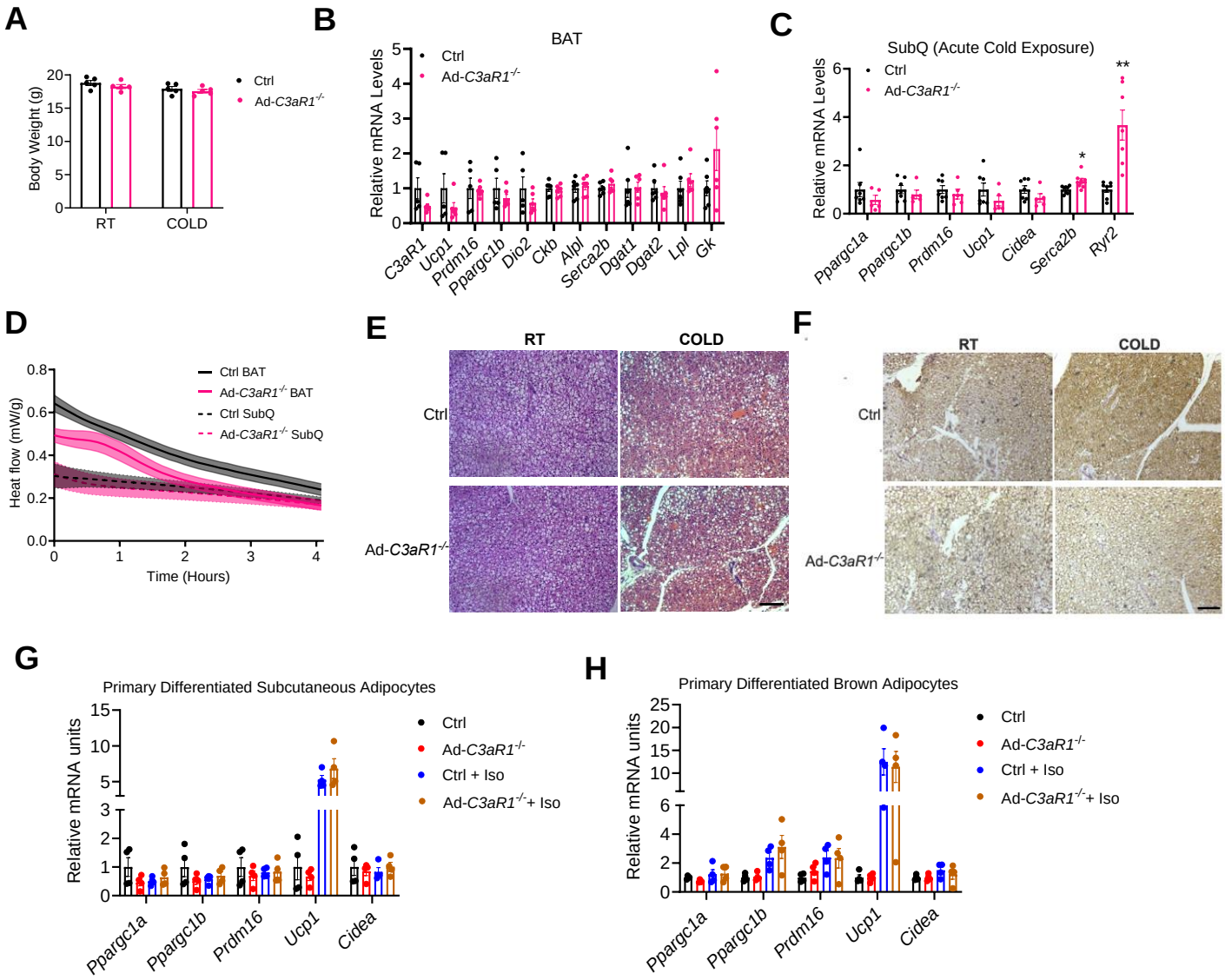

Supplemental Figure 4.

A) Body weight of control and Ad-*C3aR1* knockout female mice at room temperature and 6 hours post cold exposure. n=5/group.

B) Thermogenic gene expression in brown adipose tissue (BAT) of 10-12 week old control and Ad-*C3aR1*$^{-/-}$ female mice at room temperature. n=5-6/group.

C) Thermogenic gene expression of subcutaneous (SubQ) fat in 10-12 weeks WT and Ad-*C3aR1* knockout female mice following an acute (6 hour) cold exposure. n=5-8/group.

D) Heat flow in mW recorded from wells in duplicates containing adipose tissue from control and Ad-*C3aR1*$^{-/-}$ female mice fed a regular diet at ambient temperature. n=4/group.

E and **F)** Hematoxylin and eosin (**E**) and UCP1 (**F**) immunohistochemistry staining of brown adipose tissue (BAT) sections from 10-week-old control and Ad-*C3aR1* knockout female mice at room temperature (RT) and following acute cold exposure. Representative images are shown at 20x magnification. Scale bar, 200 μm.

G and **H)** Thermogenic gene expression in primary subcutaneous (**G**) and brown (**H**) adipocytes treated with isoproterenol (Iso) from control and Ad-*C3aR1*$^{-/-}$ female mice. n=4/group.

Data are presented as mean± S.E.M. Unpaired two-tailed t test is used for comparison. *p < 0.05, **p < 0.01.